Realistic calculations for strangeness exchange at rest

Dean Halderson
Physics Department, Western Michigan University, Kalamazoo, Michigan 49008

R. J. Philpott
Physics Department, The Florida State University, Tallahassee, Florida 32306
(Received 9 November 1987)

Calculations have been performed for the $^{12}C(K^-,\pi^-)^{12}_{\Sigma}C$, $^{12}C(K^-,\pi^+)^{12}_{\Sigma}Be$, and $^{12}C(K^-,\pi^-)^{12}_{\Lambda}C$ reactions with stopped kaons. A g-matrix YN interaction is employed in structure calculations with the recoil corrected continuum shell model. This provides a realistic prediction of the hypernuclear structure above the hyperon escape threshold. The $\Sigma N \rightarrow \Lambda N$ conversion process is treated by both absorption in the ΣN interaction and by effective lambda channels in separate calculations. Both seem to be necessary for a complete representation of capture rates. No observable structure is predicted due to substitutional states in $^{12}_{\Sigma}Be$. The substitutional states in $^{12}_{\Sigma}C$ are obscured by a large quasifree background. It is concluded that experiments based on capture of stopped kaons will not provide definitive information on the structure of Σ hypernuclei.

I. INTRODUCTION

The development of kaon beams at the Brookhaven National Laboratory Alternating Gradient Synchrotron and CERN, and the subsequent strangeness exchange experiments have produced valuable data on lambda hypernuclei.[1,2] Theoretical analyses of these data have provided information in a number of areas ranging from the baryon-baryon interaction[3] to weak decays.[4] With the discovery of long-lived, Σ-hypernuclear states by (K^-,π^-) in flight,[5,6] it was hoped that careful investigation of these states would be as fruitful in testing theories as was the investigation of lambda states. The original data for Σ hypernuclei had rather poor statistics, and although theoretical analyses were performed,[7,8] a caution was issued in Ref. 7 that better statistics were necessary for definitive conclusions.

New efforts were made to improve the experimental information by using stopped kaons (capture at rest).[9,10] In Ref. 9 a π^0-tagging procedure showed three peaks in the $^{12}C(K^-,\pi^+)^{12}_{\Sigma}Be$ spectrum above Σ^- escape threshold. Similar results were reported in Ref. 10, where a different tagging procedure was employed. Theoretical calculations[11,12] were performed to analyze this structure and conclusions were made concerning the strength of the ΣN spin-orbit interaction. It was pointed out in Ref. 11, however, that the strength of the three peaks was not consistent with their calculations. Better statistics eventually revealed[13] that no obvious structure appears in the experimental spectrum. Therefore, the (K,π) reactions have not yet provided definitive information on the spin structure of the ΣN interaction.

This paper describes some of the difficulties in making reasonable calculations for the Σ hypernuclei and presents realistic predictions for the stopped-kaon experiments. The conclusions are, first, that it is beneficial to look at the $\Sigma N \rightarrow \Lambda N$ conversion process both as an absorption in the ΣN interaction and as due to effective lambda channels. Second, the $s_{1/2}(\Sigma)$ ground state is too broad to be observed due to the $\Sigma N \rightarrow \Lambda N$ conversion process. Third, the $p_{3/2}(\Sigma^-)$ substitutional state in $^{12}_{\Sigma}Be$ is too broad to be observed due to its escape width. Fourth, the $p_{3/2}$ substitutional state in $^{12}_{\Sigma}C$ is obscured by the quasifree background.

II. CALCULATIONAL PROCEDURE

The formalism for capture at rest has been given by Hüfner, Lee, and Weidenmüller.[14] It has been thoroughly amplified by Gal and Klieb.[15] Basically, one begins by calculating the K^- capture rate to a particular hypernuclear state,

$$W_H = \int \frac{2\pi}{\hbar} \frac{1}{[l_K][J_N]} \sum_{\mu_K \mu_N \mu_H} \rho(E_f) \mid T_{fi} \mid^2 d\Omega_\pi , \tag{1}$$

where $\rho(E_f)$ is the final density of states, $[J] \equiv 2J+1$, μ_K, μ_N, and μ_H are the kaon, nuclear, and hypernuclear angular momentum projections, respectively, and

$$T_{fi} = \sum_i \int \chi^{(-)*}(\mathbf{r}_\pi)\Phi^*(\epsilon) v(\mathbf{r}_K - \epsilon_i)\Phi_N(\epsilon) \times \chi(\mathbf{r}_K) d\epsilon\, d\mathbf{r}_\pi d\mathbf{r}_K . \tag{2}$$

With the assumptions that the pion is created where the kaon is destroyed and that the interaction is of zero range, $v(r) \rightarrow t(q_f)\delta(r)$, and with the internal coordinate system of the recoil corrected continuum shell model,[16,17] (RCCSM), the transition matrix becomes[18]

$$T_{fi} = b^3 \sum_i \int \chi^{(-)*}[(M_N/M_H)\mathbf{r}_K]\Phi^*(\epsilon) t(q_f) \times \delta[\epsilon_i - b\mathbf{r}_K]\Phi(\epsilon)\chi_K(\mathbf{r}_K) d\epsilon\, d\mathbf{r}_K . \tag{3}$$

In Eq. (3), M_N/M_H is the ratio of the nuclear to hyper-

nuclear masses, $b = A/(A-1)$, where A is the atomic mass number of the target nucleus, and $\chi^{(-)}$ is the outgoing pion distorted wave, which is calculated in the present work from the optical potential of Stricker, McManus, and Carr.[19] The kaon atomic wave function $\chi(r_K)$ is taken as either the $3D$ or $2P$ wave functions of Ref. 15.

For capture to states above the hyperon escape threshold, the rate/MeV is given by[20]

$$W_H = (1/2\pi\hbar^2) \sum_{C,J_B} (\mu_C/k_C) W_{C,JB} , \tag{4}$$

where W_{C,J_B} is a fictitious capture rate calculated for Σ-wave functions with outgoing flux v_c in the open channel c. The index c stands for $\alpha J_A l j$ with J_A and j coupled to J_B, where J_A is the angular momentum of a possible core state, l and j are the Σ orbital angular momentum and total angular momentum, respectively, and α represents other quantum numbers necessary to distinguish core states.

Since the experiments measure the fraction of captured kaons which form a definite state, one must divide by the total kaon capture rate. The resulting rate per capture K^- can be written as,[14]

$$R_{if}/K^- = [\sigma^{KN\to\pi(\tau)Y}/(\sigma^{Kn}_{tot}+\sigma^{Kp}_{tot})] \times \left[W_H \Big/ \sum_h W_h \right] , \tag{5}$$

where the first factor in Eq. (5) is the ratio of the cross section for the elementary process $KN\to\pi(\tau)Y$ to the sum of Kn and Kp cross sections, and the second factor is the rate to the state H divided by the sum over all states accessible by $KN\to\pi(\tau)Y$. This second factor is called the rate per hyperon in Ref. 15, R_{if}/Y. It is the rate per hyperon which will be calculated in this paper. Estimates of the first factor in Eq. (5) are given in Ref. 15. Also found in Ref. 15 is a correction factor to account for medium modification of the elementary t matrix. This factor is omitted from this work. The reason for the separation shown in Eq. (5) is that the ratio of experimental sections can be reasonably well determined, whereas absolute rates would be less well determined.

It is possible, with some approximations, to obtain an expression for R_{if}/Y by utilizing the completeness of the sum over h.[14,15] In the notation used by the present authors the expression becomes

$$R_{if} = (J_H+1)/(2J_N+1) \sum_{lL\alpha\beta\alpha'\beta'} (2l+1)[(2j_\alpha+1)(2j_{\alpha'}+1)(2j_\beta+1)(2j_{\beta'}+1)]^{1/2} \times \langle l l_K 00 \mid L0\rangle^2 P^L_{\alpha\beta} P^L_{\alpha'\beta'} R^L_{\alpha\beta} R^L_{\alpha'\beta'} (-1)^{1-j_\beta-j_{\beta'}}/(2L+1) \times \begin{bmatrix} j_\alpha & L & j_\beta \\ -\frac{1}{2} & 0 & \frac{1}{2} \end{bmatrix} \begin{bmatrix} j_{\alpha'} & L & j_{\beta'} \\ -\frac{1}{2} & 0 & \frac{1}{2} \end{bmatrix} \Big/ \int \rho_N(br) \mid R_K(r) \mid^2 d^3r , \tag{6}$$

where

$$R^{Ll}_{\alpha\beta} = b^3 \int R_\alpha(br)[u_l(\rho_\pi)/\rho_\pi] R_K(r) R_\beta(br) r^2 dr , \tag{7}$$

$$P^L_{\alpha\beta} = \langle J_H \| [a^\dagger_\alpha + a_\beta]^L \| J_N \rangle , \tag{8}$$

$\rho_\pi = (M_N/M_H) k_\pi r$, and the kaon wave function $R_K(r)$ is normalized such that $\int \mid R_K(r) \mid^2 r^2 dr = 1$.

The primary difference between the present calculation and earlier calculations for capture at rest is the use of RCCSM wave functions for the hypernuclear states. The RCCSM generates hyperon wave functions in terms of internal coordinates by finding eigenstates of the translationally invariant Hamiltonian

$$H = H_{core} + p_\Sigma{}^2/2m_E + \sum_{i=1} V_{\Sigma N}(i) - T_{c.m.} \tag{9}$$

for any hypernuclear excitation energy, whether below or above the hyperon escape threshold. For energies above the hyperon escape threshold, the eigenstates are normalized such that one obtains the rate per hyperon per energy. Bound states, resonances, and quasifree scattering are, therefore, consistently included in the calculation, as was described in Ref. 21.

Continuum calculations using different techniques were reported in Refs. 22 and 23. The RCCSM, however, allows for coupling of many channels, removes spurious center-of-mass excitations, and also allows for a complex YN interaction. The use of a complex interaction is one method of accounting for the $\Sigma N\to\Lambda N$ conversion process. It is absolutely necessary to account for this process, if one is making predictions which can be compared to experiment, because of the increase it produces in the widths of states. In fact, it was originally believed that this conversion width was so large that sigma-hypernuclear states would not be observed.

It is at present not feasible to include the $\Sigma N\to\Lambda N$ process in a fully satisfactory manner. The difficulty is that the binary breakup process ${}^A_\Sigma Z \to {}^{A-1}Z + \Lambda$ accounts for a very small percentage of the hypernuclear conversion process. It is very much more likely that three or more reaction products are created. The use of a complex YN interaction, therefore, seems like an attractive idea. Such an interaction can incorporate the range and the spin and isospin dependence of the $\Sigma N\to\Lambda N$ process. However, the use of absorption in this manner does not properly represent the experiments performed when observing states above the sigma escape threshold. When the rate per hyperon is calculated from wave functions obtained from the Hamiltonian of Eq. (9), including absorption, it should be compared to the results of an experiment in which the outgoing pion is observed in coincidence with an outgoing sigma of the proper energy.

The absorption accounts for the loss of sigma flux due to conversion to a lambda. The measured rate per hyperon, obtained by observing just a pion of the proper energy, clearly includes other contributions as well and so is expected to be much larger and possibly broader than the calculated rate. However, the inclusion of absorption will provide the necessary estimate to the increase in widths which results from the conversion process.

For states below sigma-escape threshold, one can remedy this situation somewhat by finding complex eigensolutions of the Hamiltonian. Each complex eigenstate is normalized to unity and its width is taken to be twice the imaginary part of the corresponding eigenvalue. This normalization does not change the excitation strength much. In this paper, calculations with absorption will treat states below threshold in this manner. Above threshold the calculations with absorption are not adjusted in any way.

A second prescription for treating the $\Sigma N \rightarrow \Lambda N$ process is to employ effective lambda channels.[24] Even though the ${}^{A}_{\Sigma}Z \rightarrow {}^{A-1}Z + \Lambda$ channel accounts for only a small percentage of the hypernuclear conversion process, it may be possible to adjust the channel energies and channel coupling strengths to provide an effective simulation of the conversion process. Calculations with this procedure will also be shown below.

III. BASES AND INTERACTIONS

The basis for ${}^{12}_{\Lambda}C$ is composed of the Λ^0 coupled to the ${}^{11}C(\frac{3}{2}^-, \frac{1}{2}^-, \frac{5}{2}^-, \frac{3}{2}^-)$ states of Cohen and Kurath.[25] The ΛN interaction is that of Ref. 18. The basis for ${}^{12}_{\Sigma}C$ is composed of the Σ^+ coupled to the ${}^{11}B(\frac{3}{2}^-, \frac{1}{2}^-, \frac{5}{2}^-, \frac{3}{2}^-)$ states plus the Σ^0 coupled to the ${}^{11}C(\frac{3}{2}^-, \frac{1}{2}^-, \frac{5}{2}^-, \frac{3}{2}^-)$ states. The basis for ${}^{12}_{\Sigma}Be$ includes the Σ^- coupled to the ${}^{11}B(\frac{3}{2}^-, \frac{1}{2}^-, \frac{5}{2}^-, \frac{3}{2}^-)$ states and the Σ^0 coupled to the ${}^{11}Be(\frac{1}{2}^+, \frac{1}{2}^-, \frac{5}{2}^+, \frac{3}{2}^-)$ states. The core states for all sigma-hypernuclear calculations are those of Teeters and Kurath.[26] Experimental core state energies are used when known. When effective lambda channels are included in the sigma-hypernuclear calculations, the additional channels resulting from the Λ^0 coupled to the ${}^{11}C(\frac{3}{2}^-, \frac{1}{2}^-, \frac{5}{2}^-, \frac{3}{2}^-)$ or ${}^{11}Be(\frac{1}{2}^+, \frac{1}{2}^-, \frac{5}{2}^+, \frac{3}{2}^-)$ core states are included. This means that the 3^- excitation function for ${}^{12}_{\Sigma}C$ requires solving a 48 coupled-channels problem at every energy of interest.

The ΣN interaction is the YNG interaction of Yamamota and Bando.[27] This interaction is expressed as a sum of three Gaussians and contains central, symmetric spin-orbit, and antisymmetric spin-orbit components. The interaction is constructed by solving the ΣN-ΛN coupled channels Bethe-Goldstone equation in nuclear matter with the Nijmegen model D potential.[28] The parameters of the interaction are fitted to the resulting g-matrix elements. Because of the possibility of the sigma converting to a lambda in nuclear matter, the interaction is complex. It is also density dependent. The calculations in this paper evaluate the interaction at a Fermi momentum of 0.8 fm^{-1} as used in Ref. 27 for an ${}^{17}_{\Sigma}O$ calculation. The calculations are not sensitive to reasonable changes in the choice of Fermi momentum. In addition to the YNG interaction, the tensor component of the interaction of Ref. 11 is included.

The effective ΛN-ΣN interaction for use in the effective Λ-channels calculations is taken to be real and equal to 15 times the imaginary component of the YNG interaction. The effective ${}^{11}Be$ ground state energy is taken to be 28 MeV below the ${}^{11}B$ ground state energy in the ${}^{12}_{\Sigma}Be$ calculations, and the effective ${}^{11}C$ ground state is taken to be 28 MeV below the ${}^{11}C$ ground state energy in the ${}^{12}_{\Sigma}C$ calculations. These choices have no justification other than that they tend to produce approximately the same widths as the complex $V_{\Sigma N}$ calculations. The trade-off between the strength of the ΛN-ΣN coupling and the position of the effective Λ threshold allows a large range of choices, but most reasonable choices yield similar results. This lack of a prescription for choosing the parameters of the effective Λ-channel approach is its major drawback.

IV. RESULTS

Several calculations are presented in the figures that follow. Unless otherwise stated, all calculations shown in the figures have been folded with a Gaussian of width 1 MeV to simulate detector resolution. In Fig. 1 is shown the rate per hyperon per MeV for capture from the $2P$ orbit to states in ${}^{12}_{\Sigma}Be$ with a real interaction and only the $\Sigma^- \times {}^{11}B(\frac{3}{2}^-, \frac{1}{2}^-, \frac{5}{2}^-, \frac{3}{2}^-)$ states included in the basis. At this level of calculation, the only notable features in the figure are the 1^- state at $B_\Sigma = 3.5$ MeV and the two peaks at approximately $B_\Sigma = -1.5$ and -5 MeV. These features will be analyzed below. Figure 2 shows the same spectrum but also including the $\Sigma^0 \times {}^{11}Be(\frac{1}{2}^+, \frac{1}{2}^-, \frac{5}{2}^+, \frac{3}{2}^-)$ states. The two spectra are much the same. This is because the mixing between configurations is small and because the Σ^0 channels open approximately 6.7 MeV above the Σ^- channels. These new channels provide some additional width to the Σ^- levels above threshold, but very little. The additional Σ^0 levels contain such small admixtures of Σ^- configurations that they do not show up in the (K^-, π^+) reaction.

Shown in Fig. 3 is the same calculation as in Fig. 2,

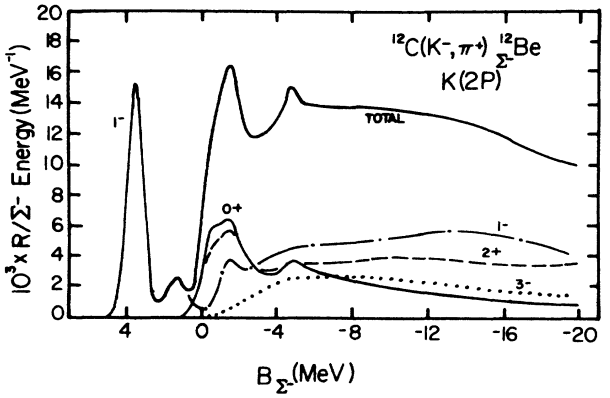

FIG. 1. Rate/Σ^-/MeV for the reaction ${}^{12}C(K^-, \pi^+){}^{12}_{\Sigma}Be$. Capture is from the atomic kaon $2P$ orbit. The interaction is real and only the $\Sigma^- \times {}^{11}B$ states are in the basis.

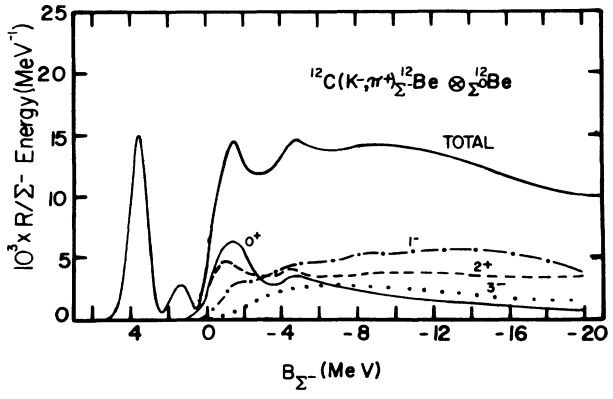

FIG. 2. Rate/Σ^-/MeV for the reaction $^{12}C(K^-,\pi^+)^{12}_{\Sigma}Be$. Same as Fig. 1 except that $\Sigma^0 \times ^{11}Be$ states are also in the basis.

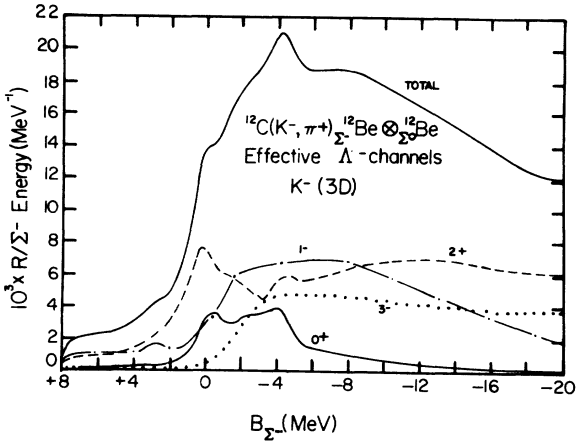

FIG. 4. Rate/Σ^-/MeV for the reaction $^{12}C(K^-,\pi^+)^{12}Be$. Same as Fig. 1 except that effective Λ channels of $\Lambda^0 \times ^{11}Be$ are in the basis.

only now the imaginary part of the interaction has been included. The 1^- states below Σ^- threshold now become a broad bump since each state has acquired a width of 6 MeV due to the complex interaction. This is a common feature of the $^{12}_{\Sigma}Be$ and $^{12}_{\Sigma}C$ calculations, i.e., the Σ-hypernuclear ground state becomes too broad to be observed in a spectrum due to the conversion process. This tendency was pointed out in Ref. 8. In addition, the structures above the Σ^- threshold are barely noticeable in the total spectrum. Their strength has also been spread. The use of the effective Λ channels described above instead of a complex interaction makes them reappear to some extent, as is shown in Fig. 4.

It is tempting to suppose that the continuum structures seen in Figs. 1–4 represent $p(p)^{-1}p(\Sigma^-)$ states. They do represent $p(\Sigma^-)$ strength, but they are not states. Instead, the $p(\Sigma^-)$ strength is being modulated by the ^{11}B thresholds in such a way as to produce peaks.

The reason for the threshold peaks can be understood by standard potential well considerations. Figure 5 displays the results of Woods-Saxon potential well calculations. The figure shows plots of $12\pi \sin^2\delta_1/k^2$ versus B_Σ for three conditions, namely, when the well depth was adjusted to produce a $p_{3/2}$ phase shift of $\pi/2$ at $B_\Sigma = -0.1$, -0.5, and -0.9 MeV. Figure 5(a) shows the

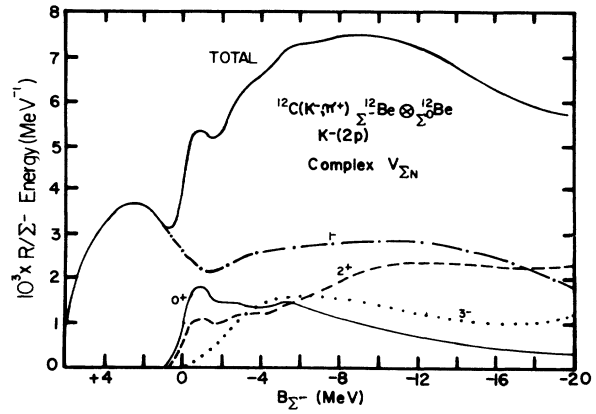

FIG. 3. Rate/Σ^-/MeV for the reaction $^{12}C(K^-,\pi^+)^{12}_{\Sigma}Be$. Same as Fig. 2 except that the interaction is complex.

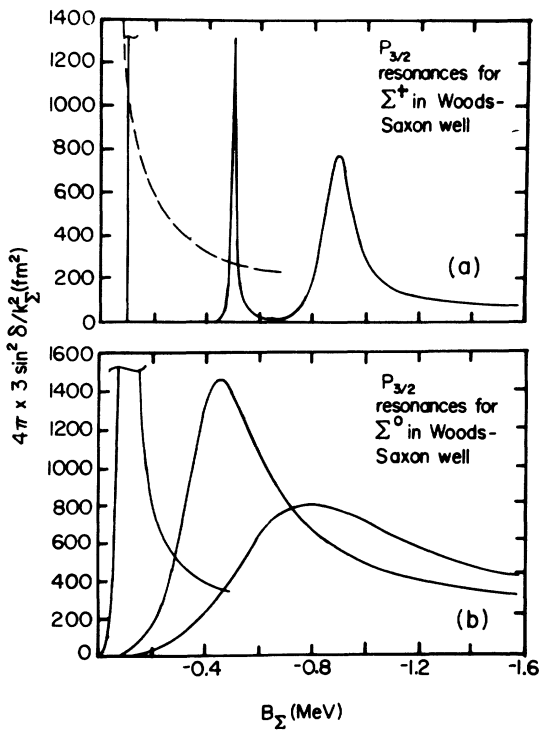

FIG. 5. (a) Solid line is $12\pi \sin^2\delta_1/k_{\Sigma^2}$ plotted vs B_{Σ^+} for Woods-Saxon well depths so as to produce 90° phase shifts for $B_{\Sigma^+} = -0.1$, -0.5, and -0.9 MeV. The dashed line is a typical result for Σ^-. (b) The solid line is $12\pi \sin^2\delta_1/k_{\Sigma^2}$ plotted vs B_{Σ^0} for a neutral sigma and Woods-Saxon well depths adjusted so as to produce 90° phase shifts at -0.1, -0.5, and -0.9 MeV.

results for Σ^+ as a solid line. Here one can see that the resonances remain narrow out to $B_\Sigma = -0.9$ MeV. This is due to the addition of the Coulomb and centrifugal barriers. Figure 5(b) shows the results for Σ^0. The $B_\Sigma = -0.9$ MeV level is now too broad to be called a resonance, and one must move the level down to $B_\Sigma = -0.5$ MeV to make it look like a resonance. Now only the centrifugal barrier is tending to hold the unbound particle inside the well. When one then places a Σ^- inside the well, the effective radial potential has no barrier, because the negative Coulomb potential has more than canceled the centrifugal barrier. If one tries to find an energy where the phase shift goes through $\pi/2$ by searching toward threshold, a clear resonance cannot be found before one runs into the atomic resonances. A typical behavior for $12\pi \sin^2\delta_1/k^2$ with Σ^- is shown as a dashed line in Fig. 5(a). This shows the characteristic threshold rise.

Conditions could exist to produce narrow Σ^- states above threshold. For instance, a $p_{3/2}$ single-particle state could mix with a state which has no escape width. But a state with no single-particle strength would not be excited in the one-step process which is assumed when one uses the distorted wave impulse approximation. If the amount of $p_{3/2}$ single-particle strength becomes large enough to allow significant excitation via a one-step reaction, then the width of the state becomes too large for the state to be observed.

Other points can be made by observing the curves in Figs. 2, 3, and 4. The first observation is that the inclusion of the imaginary part of the ΣN interaction reduces the capture strength in the $B_\Sigma = 0$ to -5 MeV region as was explained above. The second observation is that the use of effective Λ channels redistributes some of the 0^+, $p(\Sigma)$ strength from the $B_\Sigma = = -1$ MeV region to the $B_\Sigma = = -4$ MeV region. Therefore the use of effective Λ channels is capable of producing changes in the calculated structure which may not be physical.

In Fig. 6 is shown the results of a calculation equivalent to that given in Fig. 3, except that now the kaon is captured from a $3D$ orbit instead of a $2P$ orbit. One can see that there is some change in the rate, but the basic shape of the spectrum is much the same as in Fig. 3. In addition, Ref. 11 pointed out that the capture rate is almost independent of the atomic radial quantum number. Therefore the above conclusions do not depend on the specific distribution of atomic orbits.

Calculations were also performed for the rate/Σ^0/MeV in the (K^-,π^-) capture reaction. Only R_{if}/Σ^0 was calculated to correspond to the proton veto tagging procedure described in Ref. 29. In Fig. 7 is shown the results of the calculation with only the $\Sigma^0 \times {}^{11}\mathrm{C}(\frac{3}{2}^-, \frac{1}{2}^-, \frac{5}{2}^-, \frac{3}{2}^-)$ states in the basis and only the real part of the ΣN interaction. The 0^+ and 2^+ levels between $B_{\Sigma^0} = 0$ and -5 MeV are now genuine resonances; however, the spin-orbit interaction is too weak to split the $p_{3/2}(\Sigma^0) \times {}^{11}\mathrm{C}(3/2^-)$ and the $p_{1/2}(\Sigma^0) \times {}^{11}\mathrm{C}(3/2^-)$ levels. If the spin-orbit interaction were increased, the $p_{1/2}(\Sigma^0)$ level would become too broad to be recognized as a resonance. Figure 8 shows the results when the $\Sigma^+ \times {}^{11}\mathrm{B}(\frac{3}{2}^-, \frac{1}{2}^-, \frac{5}{2}^-, \frac{3}{2}^-)$ channels are included. One sees a noticeable increase in the 0^+ and 2^+ widths with this addition. This is because the new channels lie ≈ 5 MeV below the Σ^0 channels, and therefore have a larger escape width for a given value of B_{Σ^0}. With the addition of the imaginary part of the ΣN interaction, the levels gain further width, as is shown in Fig. 9. These results indicate that no chance exists to identify a $p_{3/2}$-$p_{1/2}$, spin-orbit splitting in the capture at rest spectrum.

The last graph for ${}^{12}_{\Sigma}\mathrm{C}$ is Fig. 10, which displays the calculation with effective Λ channels replacing the complex interaction. Here one can see another difficulty with the use of effective Λ channels. The 1^- ground state is much narrower than it was in the calculation that included a complex interaction. However, if this width is increased by increasing the strength of the Σ coupling interaction, the capture rate in the quasifree region increases much beyond its value in Fig. 10. The effective Λ channels are providing a nonphysical way for the sigmas to leave the nucleus. One also notes from Fig. 10 that even though the 0^+ and 2^+ structure reappears, this structure is overwhelmed by the quasifree contribution,

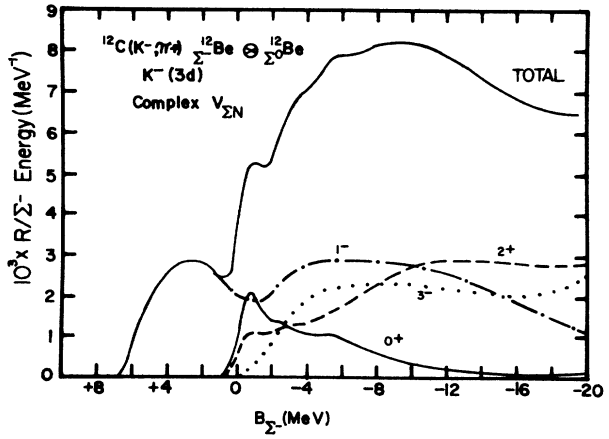

FIG. 6. Rate/Σ^-/MeV for the reaction $^{12}\mathrm{C}(\mathrm{K}^-,\pi^+)^{12}_{\Sigma}\mathrm{Be}$. Capture is from the atomic kaon $3D$ orbit. The interaction is complex and the $\Sigma^- \times {}^{11}\mathrm{B}$ and $\Sigma^0 \times {}^{11}\mathrm{Be}$ states are in the basis.

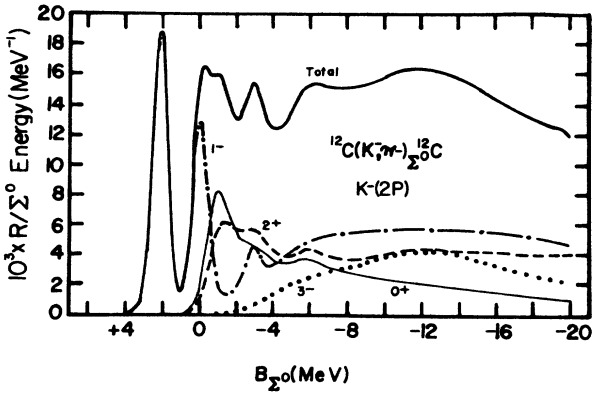

FIG. 7. Rate/Σ^0/MeV for the reaction $^{12}\mathrm{C}(\mathrm{K}^-,\pi^-)^{12}_{\Sigma}\mathrm{C}$. Capture is from the atomic kaon $2P$ orbit. The interaction is real and only the $\Sigma^0 \times {}^{11}\mathrm{C}$ states are included in the basis.

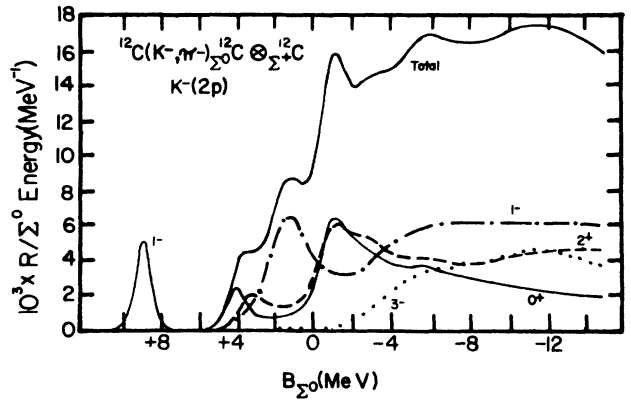

FIG. 8. Rate/Σ^0/MeV for the reaction $^{12}C(K^-,\pi^-)^{12}_{\Sigma}C$. Same as Fig. 8 except that $\Sigma^0 \times ^{11}C$ states are also in the basis.

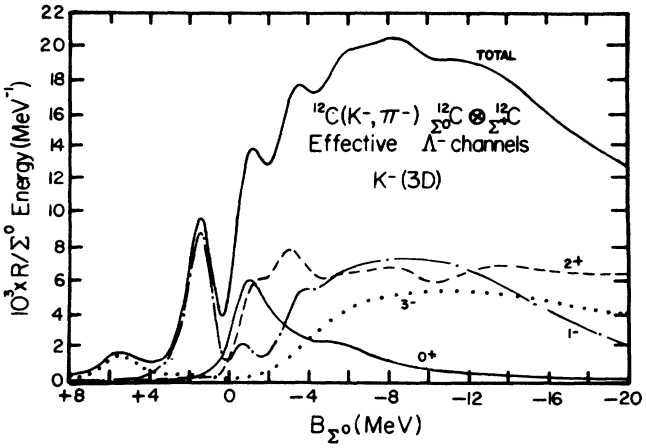

FIG. 10. Rate/Σ^0/MeV for the reaction $^{12}C(K^-,\pi^-)^{12}_{\Sigma}C$. The capture is from the atomic kaon 3D orbit. The effective lambda channels of $\Lambda^0 \times ^{11}C$ and the $\Sigma^0 \times ^{11}C$ and $\Sigma^+ \times ^{11}B$ states are in the basis.

mainly due to the 1^- and 3^- strength.

Finally, a calculation for $^{12}C(K^-,\pi^-)^{12}C$, capture at rest, is shown in Fig. 11. This figure is included so that at least one comparison can be made with data. Two data sets appear in Fig. 11.[9,10] They have been arbitrarily normalized. The dashed set of Ref. 10 is the more recent data with better statistics; however, it shows the greatest disagreement with the calculation. The disagreement is primarily in the ratio of the ground state peak to the $p(n)^{-1}p(\Lambda)$ peak. The calculation predicts a ratio of 6.6, and Ref. 10 quotes a value of 1.60 ± 0.46. Other calculations have also predicted larger values of this ratio, e.g., 4.9 in Ref. 30, and 3.4, 2.9, and 3.8 in Ref. 15. Previous calculations with the RCCSM (Refs. 18 and 21) wave functions for $^{12}C(K^-,\pi^-)^{12}_{\Lambda}C$ and $^{12}C(\pi^+,K^+)^{12}_{\Lambda}C$ in flight showed slight disagreement with experiment when comparing the equivalent ratio. This was attributed to the 2 MeV overbinding of the ground state due to omission of the three-body ΛNN force. However, the disagreement for capture at rest is significant and should be investigated further, both experimentally and theoretically.

V. CONCLUSIONS

This paper has presented calculations for K^- capture at rest leading to sigma-hypernuclear states. The calculations employed the YNG g-matrix interaction of Yamamoto and Bando.[27] Wave functions were calculated with the RCCSM (Refs. 16 and 17), and therefore, included bound states, resonances, and quasifree scattering. Two methods were employed to account for the $\Sigma N \rightarrow \Lambda N$ conversion process. First, the imaginary part of the YNG interaction was included; second, effective Λ-escape channels were included. Due to the deficiencies

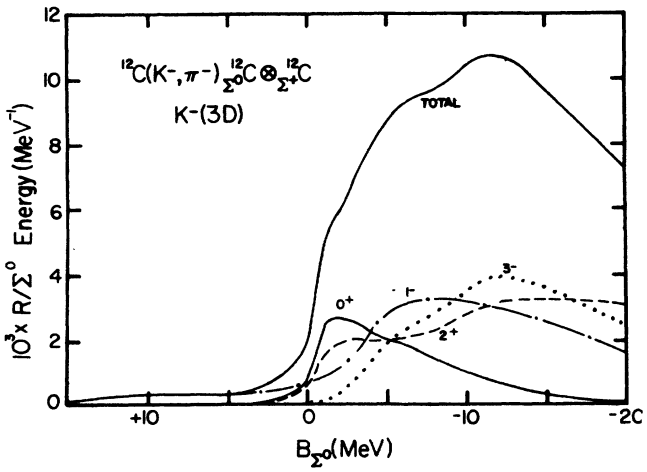

FIG. 9. Rate/Σ^0/MeV for the reaction $^{12}C(K^-,\pi^-)^{12}_{\Sigma}C$. Same as Fig. 9 except that the capture is from the atomic kaon 3D orbit and the interaction is complex.

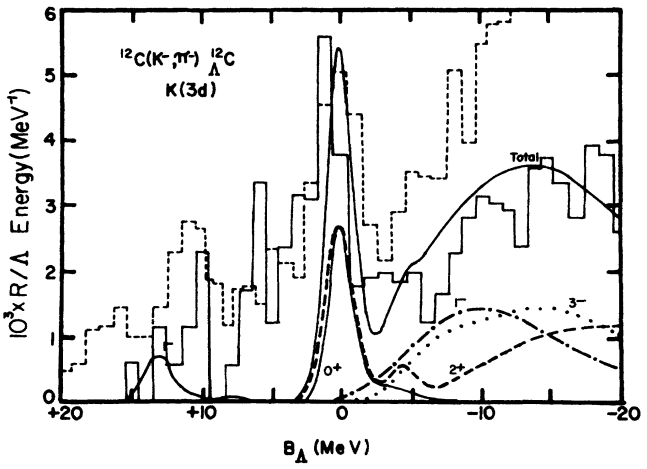

FIG. 11. Rate/Λ^0/MeV for the reaction $^{12}C(K^-,\pi^-)^{12}_{\Lambda}C$. The capture is from the atomic 3D orbit. The $\Lambda^0 \times ^{11}C$ states are in the basis. The solid histogram is the arbitrarily normalized data of Ref. 10 and the dashed histogram is the arbitrarily normalized data of Ref. 9.

of both procedures, it is beneficial to see the results of the two calculations.

Calculations were performed for $^{12}C(K^-,\pi^+)^{12}_{\Sigma}Be$. The (K^-,π^+) reaction initially seemed very attractive because it placed only a Σ^- in the nucleus, as opposed to the (K^-,π^-) reaction which could place both a Σ^0 and Σ^+ in the nucleus. However, the structure calculated in the $^{12}_{\Sigma}Be$ spectrum was determined to be due to threshold effects. The escape width of the Σ^- p wave is so large that individual substitutional states will not be observed. This means that the (K^-,π^+) reaction has very limited use in determining Σ-hypernuclear structure.

Calculations were also performed for $^{12}_{\Sigma}C(K^-,\pi^-)^{12}C$. The structure calculated in the $^{12}_{\Sigma}C$ spectrum corresponds to genuine resonances, but is obscured by the quasifree background. It therefore appears that further investigations of the sigma-hypernuclei by capture at rest will yield little additional information on the ΣN interaction. It would appear much more reasonable to pursue (K^-,π^-) in flight experiments where the energy dependence of the elementary amplitude can be exploited to separate Σ^0 and Σ^+ excitations, and one has some control over the momentum transfer to reduce the quasifree scattering.

ACKNOWLEDGMENTS

The authors would like to express their appreciation to Dr. D. Kurath for his assistance with the implementation of the wave functions in Ref. 26. These calculations were performed on the Western Michigan University FPS-264. This work was supported in part by National Science Foundation Grant No. PHY-8604375.

[1] *Proceedings of the Institue for Nuclear Study International Symposium on Hypernuclear Physics, 1986,* edited by H. Bando, O. Hashimoto, and K. Ogawa (University of Tokyo, Tokyo, 1986).

[2] *Proceedings of the International Symposium on Hypernuclear and Kaon Physics* [Nucl. Phys. **A450**, 1 (1986)].

[3] A. Bouyssy, Nucl. Phys. **A290**, 324 (1977).

[4] J. Dubach, Nucl. Phys. **A450**, 71c (1986).

[5] R. Bertini, in *Meson-Nuclear Physics—1979 (Houston),* Proceedings of the 2nd International Topical Conference on Meson-Nuclear Physics, AIP Conf. Proc. No. 54, edited by E. V. Hungerford III (AIP, New York, 1979), p. 703.

[6] B. Mayer, Nukleonika **25**, 439 (1980).

[7] C. B. Dover, A. Gal, and D. J. Millener, Phys. Lett. **138B**, 337 (1984).

[8] A. Gal and C. B. Dover, Phys. Rev. Lett. **44**, 379 (1980); **44** 962 (1980).

[9] T. Yamazaki *et al.,* Phys. Rev. Lett. **54**, 102 (1985).

[10] R. S. Hayano *et al.,* in *Proceedings of the Institute for Nuclear Study International Symposium on Hypernuclear Physics, 1986,* edited by H. Bando, O. Hashimoto, and K. Ogawa (University of Tokyo, Tokyo, 1986) p. 19.

[11] C. B. Dover, A. Gal, L. Klieb, and D. J. Millener, Phys. Rev. Lett. **56**, 119 (1986).

[12] J. Zofka, Nucl. Phys. **A450**, 165c (1986).

[13] K. Takahashi, International Symposium on Medium Energy Physics, Beijing, 1987 (unpublished).

[14] J. Hüfner, S. Y. Lee, and H. E. Weidenmüller, Nucl. Phys. **A234**, 429 (1974).

[15] A. Gal and L. Klieb, Phys. Rev. C **34**, 956 (1986).

[16] R. J. Philpott, Nucl. Phys. **A289**, 109 (1977).

[17] D. Halderson, Phys. Rev. C **30**, 941 (1984).

[18] D. Halderson, P. Ning, and R. J. Philpott, Nucl. Phys. **A458**, 605 (1986).

[19] K. Stricker, H. McManus, and J. A. Carr, Phys. Rev. C **19**, 929 (1979); J. A. Carr, Workshop on Nuclear Structure with Intermediate Energy Probes, Los Alamos Conference Proceedings No. LA-8303-C, 1981, p. 271.

[20] D. Halderson, R. J. Philpott, J. A. Carr, and F. Petrovich, Phys. Rev. C **24**, 1095; C. M. Vincent and H. T. Fortune, *ibid.* **2**, 782 (1970).

[21] D. Halderson, Y. Mo, and P. Ning, Phys. Rev. Lett. **57**, 1117 (1986).

[22] O. Morimatsu and K. Yazaki, in *Proceedings of the Institute for Nuclear Study International Symposium Hypernuclear Physics, Tokyo, 1986,* edited by H. Bando, O. Hashimoto, and K. Ogawa (University of Tokyo, Tokyo, 1986), p. 50.

[23] K. Ikeda and T. Yamada, in *Proceedings of the Institute for Nuclear Study International Symposium, Tokyo, 1986,* edited by H. Bando, O. Hashimoto, and K. Ogawa (University of Tokyo, Tokyo, 1986), p. 59.

[24] E. V. Hungerford, in *Proceedings of the Institute for Nuclear Study International Symposium on Hypernuclear Physics, Tokyo, 1986,* edited by H. Bando, O. Hashimoto, and K. Ogawa (University of Tokyo, Tokyo, 1986), p. 6.

[25] S. Cohen and D. Kurath, Nucl. Phys. **73**, 1 (1965).

[26] W. D. Teeters and D. Kurath, Nucl. Phys. **A275**, 61 (1975).

[27] Y. Yamamoto and H. Bando, Prog. Theor. Phys. Suppl. **81**, 9 (1985).

[28] J. M. Nagels, T. A. Rijken, and J. J. deSwart, Phys. Rev. D **12**, 744 (1975); **15**, 2547 (1977); **20**, 1633 (1979).

[29] T. Yamazaki *et al.,* Nucl. Phys. **A450**, 1c (1986).

[30] Quoted in Ref. 10 as a private communication from A. Matsuyama and K. Yazaki.